Optik 115, No. 5 (2004) 197–200
http://www.elsevier.de/ijleo

Optik Optics
International Journal for Light and Electron Optics

Influence of post-growth treatment on the holographic storage properties of In:Fe:$LiNbO_3$

Tao Zhang, Biao Wang, Shuangquan Fang, Yequan Zhao, Furi Ling, Wusheng Xu

Electro-Optics Technology Center, Harbin Institute of Technology, Harbin 150001, P. R. China

Abstract: The congruent In (3 mol%):Fe (0.03 wt%): $LiNbO_3$ crystal has been grown by Czochralski method in air. Some crystal samples were reduced in Li_2CO_3 powder, and others were oxidized in Nb_2O_5 powder. The defects and ions location in crystal were investigated by infrared (IR) transmission spectrum. The photorefractive properties were measured by two-wave coupling and light-induced scattering resistance experiments. In the oxidized sample, the photovoltaic effect was the dominant process during recording. However, for the as-grown sample as well as the reduced, the photorefractive effect was governed by the diffuse field and the photovoltaic field, together. In addition, the reduction treatment made the photoconductivity increase, which resulted in shorter erasure time and lower diffraction efficiency, but higher light-induced scattering resistance ability. The oxidation treatment caused the inverse effect.

Key words: In:Fe:$LiNbO_3$ – post-grown treatment – IR transmittance spectra – holographic storage properties

1. Introduction

Lithium niobate ($LiNbO_3$, LN) single crystal has been considered for extensive technological applications because of the excellent electric-optical, piezoelectric, dielectric and nonlinear optical properties of this material [1, 2]. Congruent $LiNbO_3$ exhibits Li-deficiency (48.6 mol% Li_2O), and contains a considerably large amount of intrinsic defects at particular lattice sites in the crystal. This means that there is still a lot of room to tailor the photorefractive properties of $LiNbO_3$ crystal by doping different kinds of impurities, i.e. damage-resistance elements (Mg, Zn, In, Sc etc.) and photorefractive sensitivity elements (Fe, Ce, Mn, Cu etc.). On the other hand, moderate post-growth treatment of oxidation and reduction can also change the valence state of the doped ions and the other defects distribution, therefore affect the photorefractive properties of the crystal. For example, the reduction treatment can enhance the exponential gain coefficient in Ce:Fe:LiNbO [3], increase the sensitivity in Mg:Mn:Fe:$LiNbO_3$ [4]. Optimizing $LiNbO_3$ crystal for good photorefractive properties by different dopants and post-growth treatments have attracted a lot of attention in holographic optical data storage.

In this work, we chose oxide In_2O_3 and Fe_2O_3 as doping impurities to grow doubly-doped In:Fe:$LiNbO_3$ single crystal by conventional Czochralski method, and studied the ions location in the host lattice and of the photorefractive properties of the crystal samples under different treatments (oxidation, reduction).

2. Experiments

2.1. Crystal growth and sample preparation

The congruent $LiNbO_3$ crystal with 1.5 mol% In_2O_3 and 0.03 wt% Fe_2O_3 doping was grown in an automatic diameter control system by Czochralski method at about 1240 °C. The starting materials are all ultra pure. The crystal was pulled along [001] direction from the melt in a platinum crucible at a rate of ~2 mm/h, and rotated at a rate of ~20 rpm. The growth temperature gradient above melt surface was about 35–40 °C/cm. After growth, the crystal was cooled down to room temperature at a speed of 100 °C/h, and then was polarized in another furnace where the temperature gradient was almost equal to zero with a DC electric density of 5 mA/cm^2 for 30 min. Finally the single domain crystal was y-cut into slices with the size of $10 \times 2 \times 10\,mm^3$ ($a \times b \times c$). Some of samples were buried into Li_2CO_3 powder to be reduced at 550 °C for 24 h, and some were buried into Nb_2O_5 powder to be oxidized at 1150 °C for 10 h. The (010) faces of all samples were polished to optical grade smoothness for characterization.

Received 25 December 2003; accepted 23 March 2004.

Correspondence to: T. Zhang
Fax: ++86-451-86418251
E-mail: tzhang_hit02@yahoo.com

0030-4026/04/115/05-197 $ 30.00/0

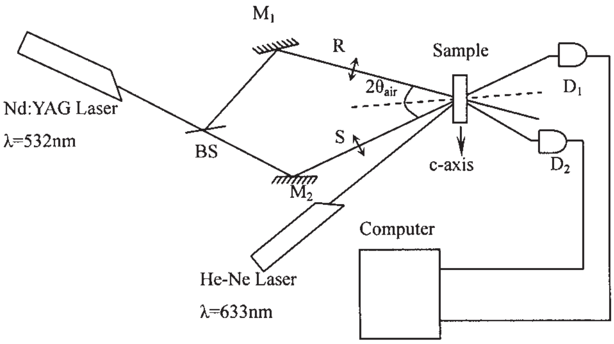

Fig. 1. Schematic diagram of two-wave coupling experimental set-up: M_1, M_2: mirrors; BS: beam splitter; D_1, D_2: detectors; R: reference beam; S: signal beam.

2.2. Characterization

The infrared transmittance spectra of the three states In:Fe:$LiNbO_3$ crystals (oxidation, as-grown and reduction) were recorded by a Fourier infrared spectrometer at room temperature. The measurement range is from 3000 cm^{-1} to 4000 cm^{-1}.

Holographic experiments were carried out by two-wave coupling at room temperature. A scheme of experimental set-up is shown in fig. 1. The holographic gratings were written by two mutually coherent and extraordinarily polarized green beams from a doubled Nd:YAG laser with the wavelength of 532 nm, i.e. signal beam S and reference beam R. The grating wave vector K of written holograms was set parallel to the crystals c axis to utilize the largest electro-optic coefficient γ_{33}. The diffraction efficiency were measured wit a He-Ne laser of weak light intensity ($\lambda = 633$ nm, ordinary polarization, $< 100\ \mu W/cm^2$).

The light-induced scattering resistance was performed with an Ar^+ laser at the wavelength of 514.5 nm. The laser incident power level could be adjusted by an attenuator. The crystal c-axis was aligned with the polarization direction of the laser beam, and placed on the back focal plane of the convex lens. The central power density of the transmitted beam was record with a detector connected with the computer. Fig. 2 shows the schematic diagram of the experiment set-up.

3. Spectroscopy

Because of H_2O vapor existing in air, H^+ was introduced into the crystal lattice and formed O-H bond during the growth of crystals. The position of doped ions could be conjectured by analyzing the change of OH^- absorption peak. Fig. 3 shows the infrared transmission spectra of the crystals.

The OH^- absorption peak of Fe (0.03 wt%):$LiNbO_3$ is located at about 3482 cm^{-1}, corresponding to the vibration of $V_{Li}{}^-$-OH; complexes [5]. While for the In:Fe:$LiNbO_3$ crystals, the treatments seem to have little influence on the absorption peaks, located in 3507, 3504 and 3508 cm^{-1}, respectively. This indicates that the In concentration in crystals is over the threshold [6, 7]. It is proposed that the In^{3+} ions over the threshold concentration firstly replace Nb^{5+} ions at Li sites, and then the additional begin to enter Nb sites forming $In_{Nb}{}^{2-}$ defects and repel $Fe_{Li}{}^{2+}$ entering Nb sites. Because $In_{Nb}{}^{2-}$ defects have a stronger force to H^+, the H^+ in the OH^--$V_{Li}{}^-$ complexes are attracted by $In_{Nb}{}^{2-}$ defects forming $In_{Nb}{}^{2-}$-OH^- complexes, which is responsible for the absorption peak at 3507 cm^{-1}.

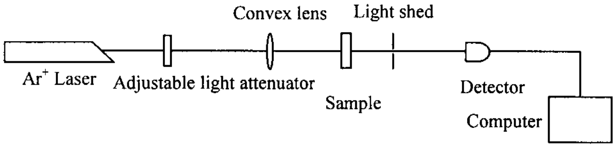

Fig. 2. Experimental set-up for measuring light-induced scattering resistance ability.

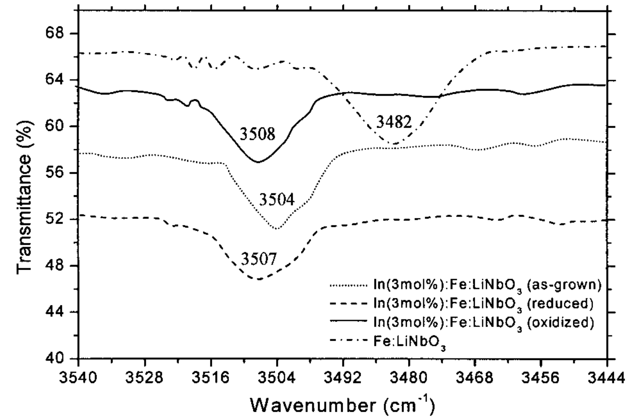

Fig. 3. IR transmittance spectra of In (3 mol%) :Fe (0.03 %) :$LiNbO_3$ under different treatments.

4. Photorefractive properties

4.1. Diffraction efficiency

The holographic gratings were written with $I_R = I_S = 300\ mW/cm^2$ and the internal crossing angle of 9.4° between the recording beams in air (see fig. 1). The diffraction efficienty η was defined as the ratio of the diffracted beam intensity I_d to the transmitted beam intensity I_t of the probe laser beam. The corresponding refractive index change Δn and the space charge field E_{SC} were calculated by Kogelnik's formula [8] and electro-optic effect, respectively. At the same time, the amplitude of the diffuse field E_d could be determined by [9].

$$E_d = \frac{2\pi k_B T}{e\Lambda}\,, \tag{1}$$

Table 1. Summary of the photorefractive properties for In:Fe:LiNbO3 under different annealing treatments.

State	$\eta_{\max}$ (%)	Δn	E_{SC} (V/cm)	E_d (V/cm)	τ_e (s)
Oxidation	14.37	3.18×10^{-5}	1.85×10^3	517	183.30
As-grown	4.64	1.78×10^{-5}	1.04×10^3	517	9.18
Reduction	2.83	1.38×10^{-5}	0.80×10^3	517	4.44

where k_B is Boltzmann's constant, e is the electron charge, T is the absolute temperature, and Λ is the grating period. The experimental results are shown in table 1.

It can be seen from table 1 that for the oxidation sate of In:Fe:LiNbO3 crystal, the space charge field E_{SC} is much bigger than the diffusion field E_d. Therefore the additional contribution to E_{SC} is obviously photovoltaic field, i.e. the photovoltaic effect ist the dominant process during recording for the state's crystal. While in the case of the reduced or as-grown, the diffuse field is comparable with the space charge field, i.e. the photorefractive effect is governed by the diffuse field and the photovoltaic field together. In addition, the oxidation state's diffraction efficiency is bigger, and the reduction state's is smaller than that of the as-grown, 14.7 and 4.64 versus 2.83.

4.2. Erasure time

The erasure of holographic gratings usually follows a monoexponential law [10]:

$$\eta^{1/2} = \eta^{1/2}_{\max} \exp\left(-t/\tau_e\right) , \qquad (2)$$

where τ_e is the grating erasure time constant. After the diffraction efficiency of holographic gratings had reached its maximum value, the signal beam S was blocked and the reference beam R was served to erase the gratings. A typical curve of the erasing process in our experiment is shown in fig. 4. The fitted τ_e are listed in table 1.

It is obvious that the erasure time constant in the oxidation sate of In:Fe:LiNbO3 crystal is much longer compared with that of the as-grown and reduced. It is believed that the increase of the [Fe^{3+}] concentration indeed decreases the carrier mobility by oxidation, so the erasure time is prolonged, up to 183.3 s. While the reduction treatment causes an inverse effect.

4.3. Dependence of photoconductivity on light intensity

The photoconductivity can be obtained from the relation [11] $\tau_e = \varepsilon\varepsilon_0/(\sigma_d + \sigma_{\text{ph}})$, where $\varepsilon\varepsilon_0$ is the dielectric constant of LiNbO3, $\sigma_d$is the dark conductivity, and σ_{ph} is the photoconductivity. Know that the holographic grating strength didn't almost decay in the darkness in our experiment, thus for these crystals σ_d could be neglected in the measurement range of light intensity, i.e. $1/\tau_e \propto \sigma_{\text{ph}}$. So the light intensity dependence of the photoconductivity can be determined by measuring the erasure time at different light intensities. The experimental results are shown in fig. 5.

It has been demonstrated that when there only exists one energy level to take part in the photorefractive process in LiNbO3, the photoconductivity is linear with the light intensity; when there exist two energy levels, the relationship between them is nonlinear [12]. Our experimental results show that $1/\tau_e$ is proportional to I, i.e. $\sigma_{\text{ph}} \propto I$. This indicates that the photorefractive process is only related to one energy level in the three states of In:Fe:LiNbO3 crystals. In addition, in the measurement range of the light intensities, the photoconductivity of the reduced In:Fe:LiNbO3 crystal is biggest, that of the as-grown bigger and that of the oxidized smallest. Larger photoconductivity will enhance the carrier mobility. The experimental data change coincides in the 4.2 section.

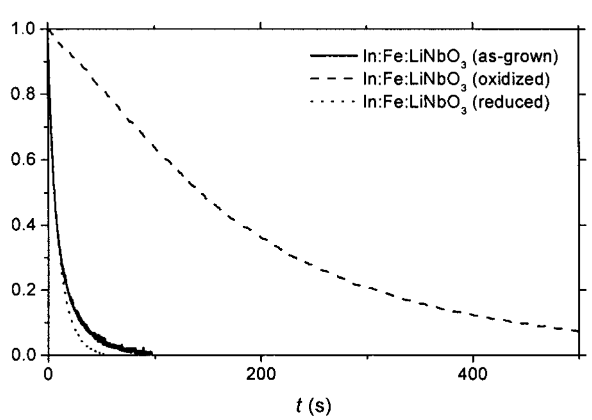

Fig. 4. Erasure curves of gratings for In:Fe:LiNbO3 under different treatments. That for Fe (0.03 wt%):LiNbO3 crystal was also plotted.

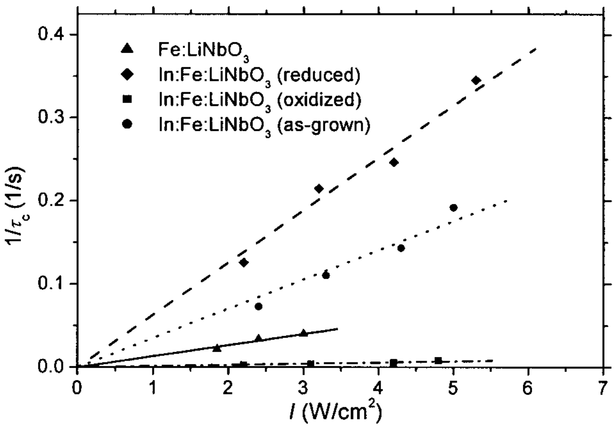

Fig. 5. Erasure time versus different light intensities. The lines are linear fits to the measured values.

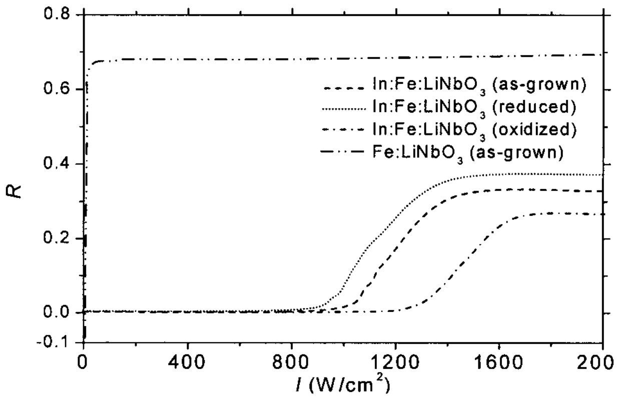

Fig. 6. Incident light intensity dependence of light-scattering noise for the different treatments of In:Fe:LiNbO$_3$ crystals. That for Fe (0.03 wt%):LiNbO$_3$ crystal was also plotted.

4.4. Light-induced scattering

The high light-induced scattering resistance ability can improve the quality of the stored information, and reduce the bit error rate. The experimental set-up is shown in fig. 2. Fig. 6 gives the ratio R of the light scattering noise intensity I' to the incident light intensity I, $R = I'/I$, in the crystals as a function of I.

From fig. 5, it can been seen that the light-induced scattering resistance ability is considerably enhanced by doping In compared to that of Fe (0.03 wt%):LiNbO$_3$ crystal, and the light-induced scattering does not occur until the incident light intensity reaches a certain value. The reduction for In:Fe:LiNbO$_3$ crystal increases the light scattering resistance ability, on the contrary the oxidation does decrease it in comparison with that of the as-grown. It is well known that the photorefraction is proportional to the ratio of the photovoltaic current to the photoconductivity. The reduction indeed increases the photoconductivity because of larger carrier mobility and less electron traps of Fe^{3+}. So the increase of the light scattering resistance ability is primarily attributed to the increase of photoconductivity.

5. Conclusions

The post-grown treatment has almost no effect on the IR absorption peaks of In:Fe:LiNbO$_3$ crystals. In the oxidized crystal, the photovoltaic effect is the dominant process during recording. While for the as-grown as well as the reduced, the photorefractive effect is governed by the diffuse field and the photovoltaic field together. The reduction treatment makes the photoconductivity increase, which results in the shorter erasure time and lower diffraction efficiency, but the higher light-induced scattering resistance ability. The oxidation treatment increases the diffraction efficiency and erasure time, but reduces the light scattering resistance ability. It is quite evident that modest treatment is of key importance for the improvement of the properties of In (3 mol%):Fe:LiNbO$_3$ crystals.

Acknowledgements. This work is financially supported by National Advanced Technology Program No. 863 (2001AA31304), the National Research for Fundamental Key Projects No. 973 (G19990330), the National Natural Science Foundation (10172030), and the Nature Science Foundation of Heilongjiang Province (A01-01), People's Republic of China.

References

[1] Fan TY, Cordova-Plaza A, Digonnet MJF, Byer RL, Shaw HJ: Nd:MgO:LiNbO$_3$ spectroscopy and laser devices. J. Opt. Soc. Am. B **3** (1986) 140–148

[2] Lallier E, Pocholle JP, Papuchon M, Mecheli M, Li MJ, He Q, Ostrowsky DB: Nd:MgO:LiNbO$_3$ waveguide laser and amplifier. Opt. Lett. **15** (1990) 682–684

[3] Yang CH, Zhao YQ, Wang R, Li MH: Studies of photorefractive crysltals of double-doped Ce, Fe:LiNbO$_3$. Opt. Commun. **175** (2000) 247–252

[4] Zhen W, Guan CX, Zhao LC, Xu YH.: The correlation of doping ions to holographic storage properties of Mg:Mn:Fe:LiNbO$_3$ crystals. J. Phys. Chem. Solids. **64** (2003) 1371–1374

[5] Schirmer OF, Thiemann O, Wohlecke M: Defects in LiNbO$_3$-I. Experimental aspects. J. Phys. Chem. Solids **52** (1991) 185–200

[6] Zhen XH, Zhang XJ, Zhao LC, Xu YH: Growth and optical properties of In:Nd:LiNbO$_3$. Solid. State. Commun. **126** (2003) 203–206

[7] Wang B, Wang R, Nie YR, Xu YH: Investigation on photorefractive properties of In:Mn:Fe:LiNbO$_3$. Opt. Matter. **23** (2003) 273–276

[8] Kogelnik H: Coupled wave theory hologram gratings. Bell Syst. Tech. J. **48** (1969) 2909–2947

[9] Volk TR, Razumovski NV, Mamaev AV, Rubinina NM: Hologram recording in Zn-doped LiNbO$_3$ crystals. J. Opt. Soc. Am. B **13** (1996) 1457–1460

[10] Hatano H, Yamaji T, Tanaka S, Furukawa Y, Kitamura K: Investigation of the oxidation state of Fe in stoichiometric Fe:LiNbO$_3$ for digital holographic recording. Jpn. J. Appl. Phys. **38** (1999) 1820–1825

[11] Chen XJ, Zhu DS, Li B, Ling T, Wu ZK: Fast photorefractive response in strongly reduced near-stoichiometric LiNbO$_3$ crystals. Opt. Lett. **26** (2001) 998–1000

[12] Buse K: Light-induced charge transport processes in photorefractive crystals I: Models and experimental methods. Appl. Phys. B **64** (1997) 273–291